The difference of the retinal structural and microvascular characteristics in patients with MOGAD-ON and AQP4-ON

Yajun Yao
Beijing Tiantan Hospital
Xindi Li
Beijing Tiantan Hospital
Yun Xu
Beijing Tiantan Hospital
Xiaofang Liang
Beijing Tiantan Hospital
Liu Yang
Beijing Tiantan Hospital
Fu-Dong Shi
Beijing Tiantan Hospital
Xinghu Zhang
Beijing Tiantan Hospital
De-cai Tian (decaitian@hotmail.com)
Beijing Tiantan Hospital https://orcid.org/0000-0002-5153-2491

Research

Keywords: Optic neuritis, MOGAD, NMOSD, OCTA

Posted Date: November 22nd, 2021

DOI: https://doi.org/10.21203/rs.3.rs-1022210/v1

Abstract

Background

Antibodies against myelin-oligodendrocyte-glycoprotein (MOG-Abs) associated disorders (MOGAD) have been recognized as a disease entity in their own right. Optic neuritis (ON) is the most common symptom in MOGAD.

Objective

To demonstrate the differences in retinal microvascular characteristics between patients with MOGAD-ON and aquaporin-4 antibody (AQP4-Ab) positive ON.

Methods

A prospective study in which optical coherence tomography (OCT) and optical coherence tomography angiography (OCTA) were used to measure retinal and microvascular parameters.

Results

22 MOGAD-ON eyes, 32 AQP4-ON eyes and 60 control eyes were included in the study. The thickness of RNFL and GCC in MOGAD-ON eyes is significantly lower than that of HC ($p < 0.001$, respectively), but comparable to AQP4-ON eyes. The vessel density in retina capillary plexus (RCP) reduced significantly in MOGAD-ON than that in AQP4-ON ($p < 0.05$, respectively). Unlike AQP4-ON, the visual accuracy in MOGAD-ON was positivitly correlated with vessel density of superficial RCP ($P = 0.010$) and ON relaspe times ($P = 0.038$).

Conclusion

The retinal neuro-axonal damages between MOGAD-ON and AQP4-ON were comparable. Unlike AQP4-ON eyes, microvascular densities were significantly reduced in MOGAD-ON, and was positively correlated with the deterioration of visual acuity in MOGAD-ON.

1. Introduction

Antibodies against myelin-oligodendrocyte-glycoprotein (MOG-Abs) have been detected in several autoimmune central nerve systems (CNS) disorders, in which the clinical characteristics often overlap with aquaporin-4 (AQP4) Ab-negative neuromyelitis optica spectrum disease (NMOSD)[1, 2]. Recently, MOG-Ab associated disorders (MOGAD) have been recognized as a disease entity in their own right due

to the immunopathology mediated by MOG-Abs[1, 3, 4]. Optic neuritis (ON) is the most common neuro-ophthalmic symptom in MOGAD, accounting for approximately 78% of MOGAD patients[5, 6]. MOGAD-ON manifests as recurrent episodes and severe visual impairment (even blindness) with optic disc swelling and extensive optic nerve lesions[7]. However, unlike NMOSD-ON with poor prognosis[8, 9], the vision acuity is often preserved in MOGAD-ON because it responds well to steroids[10].

Both optical coherence tomography (OCT) and optical coherence tomography angiography (OCTA) are non-invasive imaging techniques used to visualize the microstructures of fundus. OCT performs a real-time and in vivo retinal biopsy to directly visualize the microstructure of human eye tissue, including the peripapillary retinal nerve fiber layer (pRNFL) and ganglion cell complex (GCC)[11]. The pRNFL comprises axons originating from ganglion cell neurons and reveals optic nerve status, macular GCC is a direct reflection of the intrinsic ganglion cell bodies, which can provide information about primary retinal pathology[12]. OCTA generates high-resolution information on retinal and choroidal vessels, and gains a better visualization of vasculature around optic disc and macula[13]. As cerebral and retinal vasculatures are anatomically interconnected with similar features, a retinal vascular study would shed light on the underlying pathogenesis of microvascular impairment and neuronal damage in center nervous system.

With the utilizing of retinal OCT and OCTA into clinical neuroimmunology, researchers successively observed that pRNFL and GCC were significantly thinning in NMOSD-ON[14, 15] and MOGAD-ON[10, 16], and were consistent with their visual acuity loss. Similar to the peripapillary vascular attenuation reported in NMOSD-ON[10], the retinal vascular density also decreased in MOGAD-ON and was positively correlated with number of ON episodes[17]. Evidences above indicated that the irreversible retinal damages were not only presented in NMOSD-ON, but also in MOGAD-ON. The retinal destructions in NMOSD primarily result from the irreversible damages of AQP4-Abs to Müller cells in retina[18]. But, in MOGAD-ON, the pathologies of afferent visual system damages mediated by MOG-Ab is less well understood. As studies to compare retinal microstructures and ocular vasculature in MOGAD-ON and AQP4-Abs-positive NMOSD-ON (AQP4-ON) are limited, the severity of retinal damages following MOG-Abs and AQP4-Abs associated ON have been inconclusive. In this study, we separately investigated the retinal structural and microvascular characteristics between patients with MOGAD-ON and AQP4-ON, to demonstrate the distinct underlying pathologies of visual impairments mediated by MOG-Abs and AQP4-Abs, which is important for refining diagnoses and tailoring treatments.

2. Materials And Methods

2.1 Study participants

We performed a prospective study, Clinical and Imaging Patterns of Neuroinflammation Diseases in China (CLUE, NCT: 04106830). Patients who had a history of ON were enrolled from Jan. 2019 to Jan. 2021 in neurology department of Beijing Tiantan Hospital, Capital medical university. ON was defined as the presence of an acute relapse lasting more than 24 hours and associated with decreased high-contrast letter acuity, pain with eye movement, color desaturation and/or visual field (VF) abnormalities, with or

without optic nerve swelling or enhancement visualized by magnetic resonance imaging (MRI). Ethical approval for this study was obtained from the Institutional Ethics Committee at Beijing Tiantan Hospital.

The inclusion criteria for patients were as follows: (1) best corrected visual acuity (BCVA) of the eye with better eyesight ≥20/400, intraocular pressure (IOP) ≤ 21.0 mmHg, refraction error between +3.00 diopters; (2) without ON attack within the last two months before enrolment; (3) serum MOG-Ab or AQP4-Ab positive tested via cell-based assay (CBA); (4) able to perceive the light spot during OCT and OCT-A examinations and cooperate with the examiner. Eyes with concomitant potentially confounding diseases (glaucoma, diabetes mellitus, retinal surgery, retinal disease) were excluded. The inclusion and exclusion criteria of health controls (HCs) were similar to those for the NMOSD group except for the BCVA≥ 20/25, presence of eye diseases, and the absence of serum MOG-Ab and AQP4-Ab.

The AQP4-IgG antibody and MOG-IgG antibody testing were performed blindly at the Euroimmun Medical Diagnostic Laboratory (China) using a fixed-cell-based indirect immunofluorescence test on BIOCHIPs (EUROIMMUN AG, Lübeck, Germany). Information including demographic data, disease duration of ON, time since previous ON attack, ON relapse times and status of MOG-Abs and AQP4-Abs were collected and reviewed. The evaluation of EDSS were evaluated independently by two neurologists according to a predefined standard on the same day as the ophthalmoscopic examinations.

Early Treatment Diabetic Retinopathy Study (ETDRS) charts (Precision Vision, USA) was used to collect the prognostic Best-Corrected Distance Visual Acuity (BCVA) of the patients with ON. The presented letter-acuity scores may be converted to LogMAR (logarithm of the minimum angle of resolution) as follows: LogMAR = -(0.02) * Letters + 1.1[19]. Due to statistical availability, VA (logMAR) < 0.0 is regarded as 0.0, VA (logMAR) > 1.0 is regarded as 1.0, resulting in a range of VA (logMAR) from 0.0 (corrected decimal VA≥20/20) to 1.0 (corrected Decimal system) VA≤20/200)[20].

2.2 OCT

The thickness measurements of pRNFL, inner retina and outer retina were performed with an RTVue-XR Avanti spectral-domain OCT (Optovue, Inc., Fremont, CA, USA; software version 2017.1.0.155). Retinal imaging was firstly performed by a three-dimensional (3D) reference scan, which was used as the reference and registration image for the EMM5 macular map. It consisted of a dense grid scan in a 6x 6mm area of central macula. The optic nerve head (ONH) scan consisted of 13 concentric rings with diameter ranging from 1.3- 4.9mm and 12 radial lines with 3.4 mm length. The thickness of the retinal nerve fiber layer (RNFL) was measured at a diameter of 3.45 mm around the center of the disk using the ONH protocol. RNFL analysis was done in 8 sectors namely superotemporal (ST), superonasal (SN), inferotemporal (IT), inferonasal (IN), nasal inferior (NI), nasal superior (NS), temporal inferior (TI), and temporal superior (TS).

The perifoveal retina was divided into the inner retina and outer retina. The perifoveal retina scan is 1 mm temporal from the foveal center, and consists of 15 vertical line scans, covering a 7mm square area[21]. Ganglion cell complex (GCC) was referred to the inner retina which comprised the RNFL, the ganglion cell

layer (GCL), and the inner plexiform layer (IPL). The outer retina was measured from inner plexiform layer (IPL) to retinal pigment epithelium (RPE) layer, which consist of the inner nuclear layer (INL), outer plexiform layer (OPL), outer nuclear layer and inner segment layer (ONL+ISL), outer segment layer (OSL) and retinal pigment epithelium (RPE).

2.3 OCTA

OCTA scans of the optic disc (4.5 * 4.5 mm) and macula (6 * 6 mm) were obtained by a spectral domain system (RTVue-XR Avanti, Optovue, Fremont). The radial peripapillary capillary network was visualized on scans within a 1.0 mm wide elliptical annular region extending outward from the optic disc boundary, and the vasculature within the internal limiting membrane and the nerve fiber layer were analyzed automatically using the software.

The parafoveal capillary network was observed on scans of a circular area with a diameter of 1 mm–3 mm surrounding the fovea, while the scan of the 3 mm–6 mm annular area around the parafoveal capillaries was perifoveal capillary network. Both parafoveal and perifoveal capillary networks were further divided into superior and inferior hemisphere, temporal section (TEM), nasal section (NAS), inferior section (INF) and superior section (SUP). The superficial retinal capillary plexus (SRCP) was analyzed from 3 mm below the internal limiting membrane to the outer boundary of the IPL, and the deep retinal capillary plexus (DRCP) was referred to the layer from IPL to ONL. The vessel density was calculated as the percentage area occupied by the large vessels and micro-vessels in the analyzed region. They were automatically generated in the whole scan area and in all sections using the software (V.2017.100.0.1, Optovue, USA). The quality of OCTA images was blindly evaluated by two experienced ophthalmologists to determine interobserver reproducibility. Poor-quality images with a signal strength index less than 40 or images with residual motion artifacts were rejected.

2.4 Statistical Analysis

SPSS Statistics version 22 (IBM, Armonk, NY), and GraphPad Prism version 7.0 (GraphPad Software, La Jolla, CA) were used to analyze and created graphs. Data were presented by n (%), mean (SD) or median (range). The t-test or Mann–Whitney test were used for comparisons between demographic characteristics and clinical presentations. The generalized estimating equation (GEE) was used throughout the analysis whenever applicable for adjusting for age, gender, disease duration and the inter-eye correlation. Pearson's correlation was used to assess correlation between visual function and the parameters of OCT and OCTA parameters. A $p < 0.05$ was considered statistically significant.

3. Results

3.1 Demographic and clinical characteristics of the MOGAD-ON and AQP4-ON.

14 MOGAD-ON (22 eyes), 19 AQP4-ON (32 eyes) and 30 HC (60 eyes) participants were included in the study. The demographic and clinical features of patients and healthy controls were presented in Table 1. MOGAD-ON occurs in a similar age as AQP4-ON. The proportion of female in the MOG-ON (57.1%) was significantly lower than the proportion in AQP4-ON (89.5%, p = 0.047). The average visual accuracy of MOG-ON during the acute phase was lower than that of AQP4-ON, but it is not statistically significant (p = 0.156).

Table 1
The clinical characteristic of enrolled patients and health participants

	MOG-ON (n=14, eyes=22)	AQP4-ON (n=19, eyes=32)	HC (n=30, eyes=60)
Number of patients	14	19	30
Gender (Male / Female)	6/8*	2/17	9/21
Age (years)	36.36 (14.93)	39.00 (11.84)	38.62 (12.20)
ON history (unilateral / bilateral)	6/8	6/13	NA
Number of eyes	22	32	60
ON disease duration (mon, per eye)	28.5 (2-132)	30.0 (1.5-144)	NA
Number of ON episodes (n, per eye)	1.31 (0.57)	1.44 (0.88)	NA
Time since last ON (mon, per eye)	6 (2-132)	12 (2-144)	NA
Visual accuracy (logMAR, per eye)	0.38 (0.44)	0.66 (0.70)	NA
EDSS	3.25 (1-6.5)	4.0 (2-6.5)	NA

EDSS: expanded disability status scale; HC: health controls; MOGAD: MOG-Ab-associated disease; ON: optical neuritis; NA: not applicable.

3.2 The retinal structure and vessel density in patients with MOGAD-ON

Detailed afferent visual system parameters analyzed by OCT and OCTA were respectively summarized and compared in Table 2 and Table3. Compared with the manufacturer's normative data, the thicknesses of RNFL in all sections were reduced in 55%-86% of MOGAD eyes (Figure1) and significantly lower than HC group (p < 0.001 for all). Besides, the thickness of the inner retina and outer retina were significantly thinner in MOGAD-ON than that in HC (p < 0.001, p = 0.009, respectively).

Table 2
Retina structural data of MOGAD-ON eyes in comparison to AQP4-Ab-ON eyes and HC

	MOG-ON	AQP4-ON	HC	MOG-ON VS. AQP4-ON			MOG-ON VS. HC		
	Eye = 22	Eye = 32	Eye = 60	B	SE	p	B	SE	p
pRNFL (um)	76.95 (19.63)	77.59 (18.10)	119.74 (10.08)	-2.132	4.821	0.658	-41.783	3.175	0.000*
TEM-RNFL (um)	50.68 (18.12)	52.82 (13.06)	84.03 (9.38)	-5.446	4.138	0.188	-34.059	2.979	0.000*
SUP-RNFL (um)	93.85 (27.93)	95.50 (30.15)	146.31 (14.71)	-4.627	8.064	0.566	-51.120	4.501	0.000*
NAS-RNFL (um)	67.47 (15.56)	65.63 (13.66)	96.03 (15.68)	1.323	3.562	0.710	-27.713	3.877	0.000*
INF-RNFL (um)	94.81 (20.84)	96.20 (29.87)	152.58 (17.51)	-0.185	8.018	0.982	-55.214	5.126	0.000*
GCC (um)	74.54 (11.16)	73.06 (12.06)	99.12 (5.07)	-2.141	3.324	0.519	-23.972	1.779	0.000*
Outer Retina (um)	171.04 (6.99)	174.83 (7.64)	175.62 (7.55)	-2.115	2.290	0.356	-5.210	2.007	0.009*

AQP4-ON: aquaporin4-IgG seropositive optical neuritis; B: beta; GCC: ganglion cell complex, also refer to the inner retina; HC, health controls; INF: inferior quadrant; MOGAD: MOG-Ab-associated disease; NAS: nasal quadrant; pRNFL: peri-papillary retinal nerve fiber layer; SUP: superior quadrant; SE: standard error; TEM: temporal quadrant

Table 3
Retina angiography data of MOGAD-ON eyes in comparison to AQP4-Ab-ON eyes and health controls

	MOG-ON	AQP4-ON	HC	MOG-ON VS. AQP4-ON			MOG-ON VS. HC		
	Eye = 22	Eye = 32	Eye = 60	B	SE	p	B	SE	p
Optic disk RPC (%)	49.81 (4.95)	48.89 (6.28)	55.35 (3.82)	0.465	1.419	0.743	-4.927	0.929	0.000*
Capillary RPC (%)	42.98 (5.22)	41.64 (7.03)	51.14 (2.13)	0.590	1.568	0.707	-7.900	0.791	0.000*
Superficial retina VD									
Whole VD (%)	44.59 (5.50)	45.69 (6.48)	51.99 (2.88)	-2.758	1.444	0.056	-7.543	0.927	0.000*
Fovea (%)	13.971 (7.51)	15.28 (5.90)	19.91 (6.60)	-2.501	1.818	0.169	-6.724	1.632	0.000*
para-TEM (%)	46.65 (6.71)	47.64 (7.13)	53.31 (3.38)	-2.003	1.569	0.202	-6.454	1.055	0.000*
para-SUP (%)	47.87 (6.93)	48.86 (6.99)	54.53 (4.02)	-2.012	1.650	0.223	-6.532	1.225	0.000*
para-NAS (%)	44.86 (7.20)	47.52 (6.79)	52.83 (3.86)	-4.233	1.574	0.007*	-7.953	1.199	0.000*
para-INF (%)	45.88 (7.62)	47.41 (6.93)	53.43 (4.76)	-3.087	1.769	0.081	-7.535	1.373	0.000*
peri-TEM (%)	43.13 (4.29)	44.05 (5.56)	48.40 (2.77)	-1.806	1.170	0.123	-5.302	0.817	0.000*
peri-SUP (%)	45.17 (5.88)	46.41 (7.61)	53.09 (2.98)	-3.253	1.740	0.062	-8.105	0.962	0.000*
peri-NAS (%)	47.64 (6.70)	48.62 (6.77)	55.89 (2.77)	-2.591	1.577	0.100	-8.486	1.025	0.000*
peri-INF (%)	45.15 (6.70)	45.94 (7.76)	52.53 (3.17)	-2.586	1.950	0.185	-7.561	1.085	0.000*
Deep retina VD									
Whole VD (%)	48.76 (7.89)	53.40 (6.35)	54.84 (5.41)	-3.976	1.854	0.032*	-5.613	1.436	0.000*
Fovea (%)	29.69 (8.28)	32.28 (6.72)	37.12 (8.06)	-3.945	1.780	0.027*	-8.367	1.878	0.000*
para-TEM (%)	54.88 (8.76)	58.24 (4.82)	59.57 (3.72)	-2.064	1.653	0.212	-4.013	1.198	0.001*

	MOG-ON	AQP4-ON	HC	MOG-ON VS. AQP4-ON			MOG-ON VS. HC		
para-SUP (%)	54.22 (7.69)	57.73 (4.75)	58.25 (4.35)	-1.488	1.532	0.331	-3.323	1.219	0.006*
para-NAS (%)	54.68 (8.55)	58.14 (5.76)	59.47 (4.24)	-3.601	1.869	0.054	-4.364	1.202	0.001*
para-INF (%)	51.61 (9.00)	56.50 (6.03)	57.38 (5.32)	-3.651	1.982	0.065	-5.019	1.344	0.001*
peri-TEM (%)	52.67 (7.10)	55.36 (6.31)	57.86 (4.86)	-2.140	1.753	0.222	-4.837	1.327	0.000*
peri-SUP (%)	48.24 (10.18)	54.27 (7.56)	56.40 (6.65)	-5.254	2.349	0.025*	-7.665	1.845	0.000*
peri-NAS (%)	48.17 (9.40)	55.43 (6.06)	55.01 (6.50)	-5.380	1.965	0.006*	-6.095	1.723	0.000*
peri-INF (%)	48.68 (8.75)	53.83 (7.57)	55.21 (6.70)	-4.350	2.217	0.050	-6.012	1.750	0.001*

AQP4-ON: aquaporin4-IgG seropositive optical neuritis; B: beta; GCC: ganglion cell complex; HC, health controls; INF: inferior quadrant; MOGAD: MOG-Ab-associated disease; NAS: nasal quadrant; pRNFL: peri-papillary retinal nerve fiber layer; SUP: superior quadrant; SE: standard error; TEM: temporal quadrant; VD: vessel densities

As for the retinal vessel density between MOGAD-ON and HC, the average vessel densities of optic disk radial peripapillary capillaries (RPC) and retina in MOGAD-ON were significantly lower than that in HC ($p < 0.001$ for all, see Table 3). Moreover, the parafoveal and perifoveal vessel densities in each quadrant were also dramatically reduced in MOGAD-ON compared with HC group (Table 3).

3.3 The difference of retinal structure and vessel density between MOGAD-ON and AQP4-ON groups

The RNFL thickness of each quadrant and the thickness of the inner and outer retinal layers showing no significant difference between MOGAD-ON and AQP4-ON eyes (Figure 1 and Table 2). In term of superficial retinal capillary plexus (SRCP), the nasal parafoveal vessel densities were significantly decreased in MOGAD-ON eyes compared to AQP4-ON eyes (B = -4.233, SE = 1.574, p = 0.007, Table3). As for the deep retina capillary plexus (DRCP), the whole vessel density and perifoveal vessel densities in foveal, superior and nasal area were significantly decreased in the MOGAD-ON eyes than that in AQP4-ON eyes (p = 0.032, p = 0.027, p = 0.025, p = 0.006, respectively, Table3).

3.4 The correlation analysis between OCTA and OCT parameters in ON episodes.

GEE analyses were adjusted for age, gender, disease duration and relapse times of ON, and revealed that the superficial retinal vessel densities of all sectors were positively correlated with the thickness of RNFL

and inner retina layer in all patients. The whole deep retinal vessel densities, as well as parafoveal and perifoveal vessel densites in some sectors were also significantly positively correlated with the thickness of outer retina layer (Table 4).

Table 4
the correlation between OCT angiography parameters and OCT parameters in ON

	RNFL Average			Inner Retina (GCC)			Outer Retina		
	B	SE	p	B	SE	p	B	SE	p
Superficial retinal capillary plexus									
Whole VD (%)	0.181	0.399	0.000*	0.238	0.059	0.000*	0.022	0.114	0.850
Fovea (%)	0.138	0.057	0.015*	0.199	0.081	0.014*	-0.298	0.136	0.029*
para-TEM (%)	0.171	0.048	0.000*	0.197	0.071	0.006*	-0.012	0.127	0.925
para-SUP (%)	0.168	0.048	0.000*	0.199	0.072	0.005*	0.015	0.128	0.910
para-NAS (%)	0.168	0.047	0.000*	0.179	0.714	0.012*	0.122	0.125	0.328
para-INF (%)	0.165	0.052	0.002*	0.254	0.073	0.001*	0.126	0.135	0.352
peri-TEM (%)	0.116	0.038	0.002*	0.192	0.054	0.000*	0.005	0.095	0.960
peri-SUP (%)	0.242	0.044	0.000*	0.293	0.069	0.000*	-0.058	0.136	0.671
peri-NAS (%)	0.199	0.421	0.000*	0.232	0.065	0.000*	-0.001	0.122	0.993
peri-INF (%)	0.228	0.052	0.000*	0.341	0.072	0.000*	0.094	0.145	0.517
Deep retinal capillary plexus									
Whole VD (%)	0.044	0.054	0.412	0.045	0.772	0.563	0.241	0.122	0.048*
Fovea (%)	0.142	0.059	0.015*	0.149	0.084	0.074	-0.180	0.134	0.178
para-TEM (%)	0.045	0.057	0.427	-0.063	0.079	0.425	0.187	0.123	0.127
para-SUP (%)	0.002	0.054	0.963	-0.100	0.074	0.174	0.259	0.112	0.021*
para-NAS (%)	0.024	0.058	0.681	-0.072	0.081	0.374	0.269	0.132	0.041*
para-INF (%)	-0.014	0.064	0.827	-0.101	0.089	0.257	0.302	0.135	0.025*
peri-TEM (%)	0.034	0.055	0.544	0.028	0.079	0.725	0.171	0.119	0.150
peri-SUP (%)	0.067	0.747	0.368	0.011	0.106	0.919	0.285	0.160	0.075
peri-NAS (%)	-0.005	0.068	0.943	-0.070	0.096	0.462	0.327	0.142	0.021*
peri-INF (%)	0.069	0.066	0.294	0.058	0.093	0.533	0.305	0.139	0.028*

B: beta; GCC: ganglion cell complex; INF: inferior quadrant; NAS: nasal quadrant; pRNFL: peri-papillary retinal nerve fiber layer; SUP: superior quadrant; SE: standard error; TEM: temporal quadrant; VD: vessel densities

3.5 The correlation analysis between visual function and the parameters of OCT and OCTA

In MOGAD-ON, the LogMAR was significantly correlated with the average pRNFL thickness (r = -0.571, P = 0.006), average inner retina thickness (r = -0.593, P = 0.004), and the average vessel density of superficial retina (r = -0.578, P = 0.006), Figure 2). After adjusted for the RNFL and inner retina thicknesses and potential interactions with ON, the LogMAR was significantly correlated with vessel density of superficial retina capillary plexus (GEE B = -0.031, SE = 0.012, P = 0.010) and ON relaspe times (GEE B = 0.166, SE = 0.080, P = 0.038).

As for AQP4-ON, the LogMAR was significantly related to the average pRNFL thickness (r = -0.714, P < 0.001), average inner retina thickness (r = 0.849, P < 0.001), the average vessel density of superficial retina (r = -0.777, P < 0.001) and average vessel density of deep retina (r = -0.443, P = 0.011). In adjusted GEE models, the LogMAR was significantly related to the thickness of inner retina layer (GEE B = -0.051, SE = 0.010, P < 0.001), rather than any retinal vessel density.

4. Discussion

In this study, we mainly demonstrated differences of retinal microstructure and vasculature between MOGAD-ON and AQP4-ON. MOGAD-ON eyes presented with severe thinning of RNFL, the extent and quadrant of which were comparable to eyes with AQP4-ON. The vessel densities of DRCP in macular area of MOGAD-ON eyes were significantly lower than that of AQP4-ON eyes. Furthermore, the reduced microvascular densities were positively correlated with the deterioration of the visual acuity in MOGAD-ON.

MOGAD has gradually been a separate disease entity from NMOSD as the distinct pathologies mediated by MOG-Abs. In previous studies, changes of the retinal structure in MOGAD eyes and NMOSD eyes have been separately described[22, 23]. Consistent with the previous observations of pRNFL thinning and ganglion cell loss in MOGAD, we also described that the average thickness of RNFL in MOGAD-ON eyes was significantly lower than that in normal eyes. It is indicated that the apoptosis of retina ganglion cells and the retrograde degeneration of its axons existed in MOGAD-ON eyes.

However, OCT findings regarding the comparison of retinal microstructure changes between MOGAD-ON and AQP4-ON eyes have been inconclusive. Some studies have shown that compared with AQP4-Ab-positive NMOSD, MOGAD-ON leaded to less severe retinal damages[24, 25], but others including us found comparable thinning of the RNFL and GCIPL between these two groups[16, 22]. AQP4-Abs could directly attack AQP4 proteins highly expressed on the surface of Müller cells (mainly located in the INL) and astrocytes (mainly located in the RNFL) [18]. Müller cells are involved in various homeostatic functions of the retina. The loss of AQP4 reduces the capability of Müller cells to maintain osmotic pressure and induces retinal inflammation, leading to irreversible damages to the retina[26]. Unlike AQP4, MOG is a myelin protein specifically expressed at the outermost surface of myelin sheaths and oligodendrocyte membranes[27], and the autoimmune response to MOG cause demyelination[28]. The retinal ganglion cells are myelinated by oligodendrocytes when the bundle passes through the lamina cribrosa[29]. Consequently, retinal changes observed in MOGAD are expected to be a retrograde degenerative process.

The OCTA data regarding MOG-Ab associated retinal vessels degeneration are scarce. In conformity with previous study[17], the microvascular densities of SRCP and DRCP in MOGAD eyes were significantly lower than that of normal eyes. We further found out that retinal microvascular densities, especially in the DRCP, were significantly lower in MOGAD than in AQP4-Abs-ON. Similar to previous studies[30], the whole deep retinal vessel densities were also significantly positively correlated with the thickness of outer retina layer. The retinal microcirculation are high oxygen extraction systems whose flow is related with local neuronal activity[31]. The density of the capillary plexus used for oxygen diffusion in retina is more compressed in the deep layer than surface layer[9], thus any insult to it could lead to vascular retinal abnormalities. The retinal blood vessels share similar anatomic, physiological, and embryological characteristics to the cerebral vessels. It seems to indicate that the presence of MOG-Ab may be related to more severe vascular damages. A case of MOGAD presented with primary CNS vasculitis with perivascular inflammatory cell infiltration[32]. And another study confirmed that all vessels in MOG-Abs related demyelinating lesions were accompanied by macrophages during the acute phase, which was clearly different from AQP4-Abs-positive NMOSD[33]. Therefore, we speculate that MOG-Abs might cause the retinal destruction and degeneration by leading the peri-microvascular inflammation, rather than directly damaging retinal ganglion cells and their axons.

MOGAD-ON relatively preserved visual acuity compared with AQP4-ON, even if the severity of retinal damages was similar[34]. Unlike AQP4-IgG seropositivity ON, poor visual accuracy was related to changes of retinal structure and function[34], the deterioration visual accuracy in MOGAD patients was related with the reduction of microvascular density of SRCP after adjusting the correlation. The visual stimulation can increase neural activity and cerebral blood flow under normal physiological conditions[35]. Therefore, we speculate that when the retinal microvascular structure was damaged by inflammatory or any other pathologies, retinal perfusion becomes insufficient and affects the activity of retinal ganglion cells and causes photoreceptor damages in MOGAD-ON.

The limitations of our study mainly included that the sample size was relatively small, which is expected given the rarity of these conditions. Whether the vascular changes precede the changes of retinal structure or secondary to retinopathy cannot be proved. In addition, we didn’t include eyes that were positive for MOG-Ab and AQP4-Ab because "double positive" cases were extremely rare.

In conclusion, the retinal neuro-axonal damages in MOGAD-ON were comparable to AQP4-Abs-positive ON. Compared to AQP4-Abs, the MOG-Abs might be related to more severe vascular damages. And the reduced microvascular densities were positively correlated with the deterioration of the visual acuity in patients with MOGAD-ON. Here, we stressed the different pathophysiology between MOGAD-ON and AQP4-ON, but mechanisms by which MOG-Abs destroys the retinal structure and function is still unclear.

List of abbreviation

Antibodies against myelin-oligodendrocyte-glycoprotein, MOG-Abs; Antibodies against myelin-oligodendrocyte-glycoprotein associated disorders, MOGAD; Aquaporin-4 antibody, AQP4-Ab; Best-Corrected Distance Visual Acuity, BCVA; Central nerve systems, CNS; Cell-based assay, CBA; Deep retinal

capillary plexus, DRCP; Early Treatment Diabetic Retinopathy Study, ETDRS; Ganglion cell layer, GCL; Ganglion cell complex, GCC; Health controls, HCs; Inner nuclear layer, INL; inner segment layer, ISL; Inner plexiform layer, IPL; Inferonasal, IN; Inferotemporal, IT; Inferior section, INF; Magnetic resonance imaging, MRI; Neuromyelitis optica spectrum disease, NMOSD; Nasal section, NAS; Nasal inferior, NI; Nasal superior, NS; Optic neuritis, ON; Optical coherence tomography, OCT; Optical coherence tomography angiography, OCTA; Optic nerve head, ONH; Outer plexiform layer, OPL; Outer nuclear layer, ONL; Outer segment layer, OSL; Peripapillary retinal nerve fiber layer, pRNFL; Retina capillary plexus, RCP; Retinal pigment epithelium, RPE; Retinal nerve fiber layer, RNFL; Radial peripapillary capillaries, RPC; Superotemporal, ST; Superonasal, SN; Superior section, SUP; Superficial retinal capillary plexus, SRCP; Three-dimension, 3D; Temporal inferior, TI; Temporal superior, TS; Temporal section, TEM; Visual field, VF.

Declarations

Funding statement: Work in the authors' laboratories was supported in part by grants from National Natural Science Foundation of China (Grant numbers 81801199).

Conflict of interest: The authors declare that the research was conducted in the absence of any commercial or financial relationships that could be construed as a potential conflict of interest.

Author contribution: D.-C. T. formulated the conception and design of this study; all authors contributed to acquisition and analysis of data, and to critical revisions of the manuscript; Y.-J.Y. and X.-D.L. drafted the manuscript and prepared the figures.

Financial Disclosure: No disclosure.

Ethics Declaration: Ethical approval for this study was obtained from the Institutional Ethics Committee at Beijing Tiantan Hospital (KY2019-050-02).

References

1. Reindl M, Waters P: **Myelin oligodendrocyte glycoprotein antibodies in neurological disease**. *Nature reviews Neurology* 2019, **15**(2):89–102.
2. Kitley J, Waters P, Woodhall M, Leite MI, Murchison A, George J, Küker W, Chandratre S, Vincent A, Palace J: **Neuromyelitis optica spectrum disorders with aquaporin-4 and myelin-oligodendrocyte glycoprotein antibodies: a comparative study**. *JAMA neurology* 2014, **71**(3):276–283.
3. Jarius S, Metz I, König FB, Ruprecht K, Reindl M, Paul F, Brück W, Wildemann B: **Screening for MOG-IgG and 27 other anti-glial and anti-neuronal autoantibodies in 'pattern II multiple sclerosis' and brain biopsy findings in a MOG-IgG-positive case**. *Multiple sclerosis (Houndmills, Basingstoke, England)* 2016, **22**(12):1541–1549.
4. Lucchinetti CF, Guo Y, Popescu BF, Fujihara K, Itoyama Y, Misu T: **The pathology of an autoimmune astrocytopathy: lessons learned from neuromyelitis optica**. *Brain pathology (Zurich, Switzerland)*

2014, **24**(1):83–97.

5. Wang L, ZhangBao J, Zhou L, Zhang Y, Li H, Li Y, Huang Y, Wang M, Lu C, Lu J *et al*: **Encephalitis is an important clinical component of myelin oligodendrocyte glycoprotein antibody associated demyelination: a single-center cohort study in Shanghai, China**. *Eur J Neurol* 2019, **26**(1):168–174.
6. Ducloyer JB, Caignard A, Aidaoui R, Ollivier Y, Plubeau G, Santos-Moskalyk S, Porphyre L, Le Jeune C, Bihl L, Alamine S *et al*: **MOG-Ab prevalence in optic neuritis and clinical predictive factors for diagnosis**. *The British journal of ophthalmology* 2020, **104**(6):842–845.
7. Zhou L, Huang Y, Li H, Fan J, Zhangbao J, Yu H, Li Y, Lu J, Zhao C, Lu C *et al*: **MOG-antibody associated demyelinating disease of the CNS: A clinical and pathological study in Chinese Han patients**. *Journal of neuroimmunology* 2017, **305**:19–28.
8. Wingerchuk DM, Banwell B, Bennett JL, Cabre P, Carroll W, Chitnis T, de Seze J, Fujihara K, Greenberg B, Jacob A *et al*: **International consensus diagnostic criteria for neuromyelitis optica spectrum disorders**. *Neurology* 2015, **85**(2):177–189.
9. Kwapong WR, Peng C, He Z, Zhuang X, Shen M, Lu F: **Altered Macular Microvasculature in Neuromyelitis Optica Spectrum Disorders**. *American journal of ophthalmology* 2018, **192**:47–55.
10. Ramanathan S, Reddel SW, Henderson A, Parratt JD, Barnett M, Gatt PN, Merheb V, Kumaran RY, Pathmanandavel K, Sinmaz N *et al*: **Antibodies to myelin oligodendrocyte glycoprotein in bilateral and recurrent optic neuritis**. *Neurology(R) neuroimmunology & neuroinflammation* 2014, **1**(4):e40.
11. Lamirel C: **Optical Coherence Tomography**. In: *Encyclopedia of the Neurological Sciences (Second Edition).* Edited by Aminoff MJ, Daroff RB. Oxford: Academic Press; 2014: 660-668.
12. Jeong IH, Kim HJ, Kim NH, Jeong KS, Park CY: **Subclinical primary retinal pathology in neuromyelitis optica spectrum disorder**. *Journal of neurology* 2016, **263**(7):1343–1348.
13. Pellegrini M, Vagge A, Ferro Desideri LF, Bernabei F, Triolo G, Mastropasqua R, Del Noce CD, Borrelli E, Sacconi R, Iovino C *et al*: **Optical Coherence Tomography Angiography in Neurodegenerative Disorders**. *J Clin Med* 2020, **9**(6).
14. Vabanesi M, Pisa M, Guerrieri S, Moiola L, Radaelli M, Medaglini S, Martinelli V, Comi G, Leocani L: **In vivo structural and functional assessment of optic nerve damage in neuromyelitis optica spectrum disorders and multiple sclerosis**. *Scientific reports* 2019, **9**(1):10371.
15. Bennett JL, de Seze J, Lana-Peixoto M, Palace J, Waldman A, Schippling S, Tenembaum S, Banwell B, Greenberg B, Levy M *et al*: **Neuromyelitis optica and multiple sclerosis: Seeing differences through optical coherence tomography**. *Multiple sclerosis (Houndmills, Basingstoke, England)* 2015, **21**(6):678–688.
16. Sotirchos ES, Filippatou A, Fitzgerald KC, Salama S, Pardo S, Wang J, Ogbuokiri E, Cowley NJ, Pellegrini N, Murphy OC *et al*: **Aquaporin-4 IgG seropositivity is associated with worse visual outcomes after optic neuritis than MOG-IgG seropositivity and multiple sclerosis, independent of macular ganglion cell layer thinning**. *Multiple sclerosis (Houndmills, Basingstoke, England)* 2020, **26**(11):1360–1371.

17. Yu J, Huang Y, Quan C, Zhou L, ZhangBao J, Wu K, Zong Y, Zhou X, Wang M: **Alterations in the Retinal Vascular Network and Structure in MOG Antibody-Associated Disease: An Optical Coherence Tomography Angiography Study**. *Journal of neuro-ophthalmology: the official journal of the North American Neuro-Ophthalmology Society* 2020.
18. Hokari M, Yokoseki A, Arakawa M, Saji E, Yanagawa K, Yanagimura F, Toyoshima Y, Okamoto K, Ueki S, Hatase T *et al*: **Clinicopathological features in anterior visual pathway in neuromyelitis optica**. *Annals of neurology* 2016, **79**(4):605–624.
19. Holladay JT: **Visual acuity measurements**. *J Cataract Refract Surg* 2004, **30**(2):287–290.
20. Akaishi T, Takeshita T, Himori N, Takahashi T, Misu T, Ogawa R, Kaneko K, Fujimori J, Abe M, Ishii T *et al*: **Rapid Administration of High-Dose Intravenous Methylprednisolone Improves Visual Outcomes After Optic Neuritis in Patients With AQP4-IgG-Positive NMOSD**. *Front Neurol* 2020, **11**:932.
21. Dhasmana R, Sah S, Gupta N: **Study of Retinal Nerve Fibre Layer Thickness in Patients with Diabetes Mellitus Using Fourier Domain Optical Coherence Tomography**. *Journal of clinical and diagnostic research: JCDR* 2016, **10**(7):Nc05-09.
22. Pache F, Zimmermann H, Mikolajczak J, Schumacher S, Lacheta A, Oertel FC, Bellmann-Strobl J, Jarius S, Wildemann B, Reindl M *et al*: **MOG-IgG in NMO and related disorders: a multicenter study of 50 patients. Part 4: Afferent visual system damage after optic neuritis in MOG-IgG-seropositive versus AQP4-IgG-seropositive patients**. *Journal of neuroinflammation* 2016, **13**(1):282.
23. Zhao G, Chen Q, Huang Y, Li Z, Sun X, Lu P, Yan S, Wang M, Tian G: **Clinical characteristics of myelin oligodendrocyte glycoprotein seropositive optic neuritis: a cohort study in Shanghai, China**. *Journal of neurology* 2018, **265**(1):33–40.
24. Akaishi T, Sato DK, Nakashima I, Takeshita T, Takahashi T, Doi H, Kurosawa K, Kaneko K, Kuroda H, Nishiyama S *et al*: **MRI and retinal abnormalities in isolated optic neuritis with myelin oligodendrocyte glycoprotein and aquaporin-4 antibodies: a comparative study**. *Journal of neurology, neurosurgery, and psychiatry* 2016, **87**(4):446–448.
25. Akaishi T, Kaneko K, Himori N, Takeshita T, Takahashi T, Nakazawa T, Aoki M, Nakashima I: **Subclinical retinal atrophy in the unaffected fellow eyes of multiple sclerosis and neuromyelitis optica**. *Journal of neuroimmunology* 2017, **313**:10–15.
26. Pannicke T, Wurm A, Iandiev I, Hollborn M, Linnertz R, Binder DK, Kohen L, Wiedemann P, Steinhäuser C, Reichenbach A *et al*: **Deletion of aquaporin-4 renders retinal glial cells more susceptible to osmotic stress**. *J Neurosci Res* 2010, **88**(13):2877–2888.
27. Lebar R, Baudrimont M, Vincent C: **Chronic experimental autoimmune encephalomyelitis in the guinea pig. Presence of anti-M2 antibodies in central nervous system tissue and the possible role of M2 autoantigen in the induction of the disease**. *Journal of autoimmunity* 1989, **2**(2):115–132.
28. Weber MS, Derfuss T, Metz I, Brück W: **Defining distinct features of anti-MOG antibody associated central nervous system demyelination**. *Ther Adv Neurol Disord* 2018, **11**:1756286418762083.
29. Kels BD, Grzybowski A, Grant-Kels JM: **Human ocular anatomy**. *Clinics in dermatology* 2015, **33**(2):140–146.

30. Huang Y, Zhou L, ZhangBao J, Cai T, Wang B, Li X, Wang L, Lu C, Zhao C, Lu J *et al*: **Peripapillary and parafoveal vascular network assessment by optical coherence tomography angiography in aquaporin-4 antibody-positive neuromyelitis optica spectrum disorders**. *The British journal of ophthalmology* 2019, **103**(6):789–796.
31. Noonan JE, Lamoureux EL, Sarossy M: **Neuronal activity-dependent regulation of retinal blood flow**. *Clinical & experimental ophthalmology* 2015, **43**(7):673–682.
32. Baba T, Shinoda K, Watanabe M, Sadashima S, Matsuse D, Isobe N, Yamasaki R, Kaneko K, Takahashi T, Iwaki T *et al*: **MOG antibody disease manifesting as progressive cognitive deterioration and behavioral changes with primary central nervous system vasculitis**. *Multiple sclerosis and related disorders* 2019, **30**:48–50.
33. Takai Y, Misu T, Kaneko K, Chihara N, Narikawa K, Tsuchida S, Nishida H, Komori T, Seki M, Komatsu T *et al*: **Myelin oligodendrocyte glycoprotein antibody-associated disease: an immunopathological study**. *Brain: a journal of neurology* 2020, **143**(5):1431–1446.
34. Patterson K, Iglesias E, Nasrallah M, González-Álvarez V, Suñol M, Anton J, Saiz A, Lancaster E, Armangue T: **Anti-MOG encephalitis mimicking small vessel CNS vasculitis**. *Neurology(R) neuroimmunology & neuroinflammation* 2019, **6**(2):e538.
35. Li B, Freeman RD: **Neurometabolic coupling between neural activity, glucose, and lactate in activated visual cortex**. *Journal of neurochemistry* 2015, **135**(4):742–754.

Figures

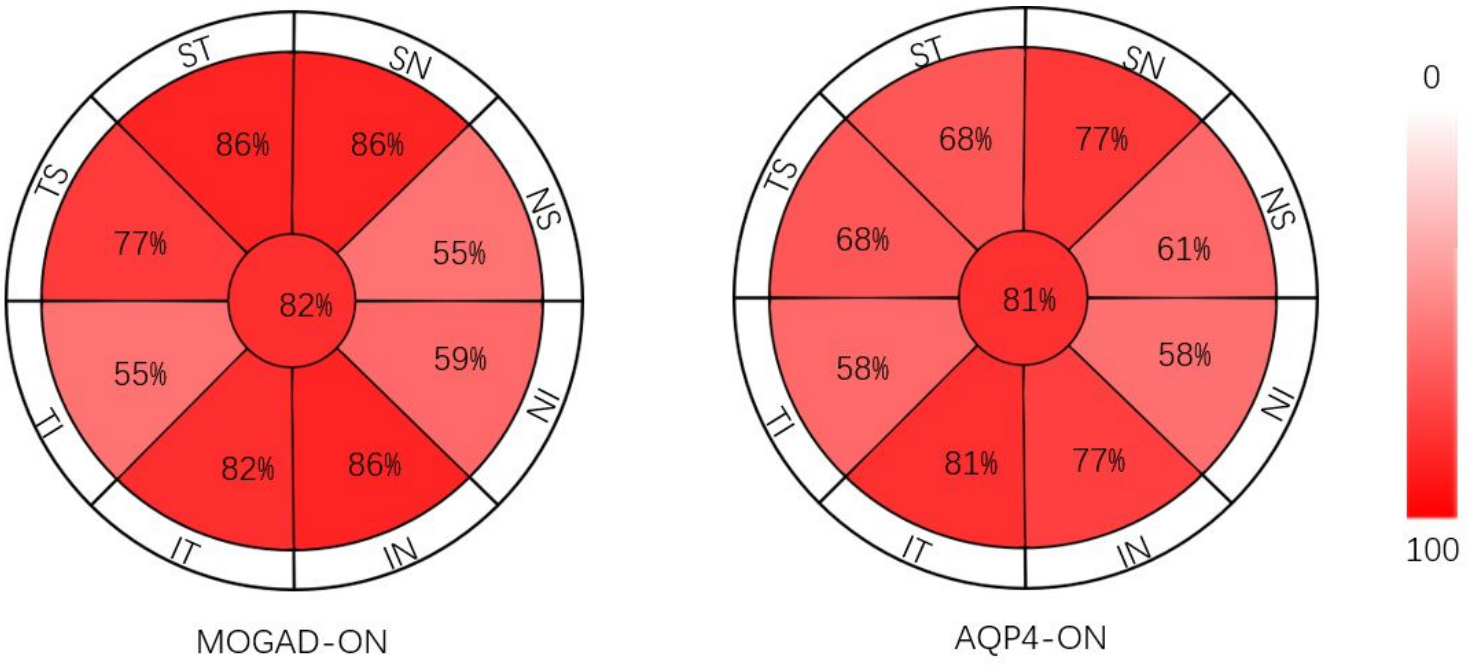

Figure 1

The proportion of eyes with reduced RNFL in each quadrant (MOGAD-ON and AQP4-ON) Compared with the manufacturer's specification data, MOGAD-ON eyes with reduced thickness of RNFL in different quadrants accounted for 55%-86%. AQP4-ON eyes with reduced thickness of RNFL in different quadrants accounted for 58%-81%. Among them, the proportion of eyes with decreased RNFL in TS, ST, SN, IT and IN were higher than other areas. TS: temporal-superior quadrant; ST: superior-temporal quadrant; SN: superior-nasal quadrant; NS: nasal-superior quadrant; NS: nasal-superior quadrant; IN: inferior-nasal quadrant; NI: nasal-inferior quadrant; IT: inferior-temporal quadrant; TI: temporal-inferior quadrant.

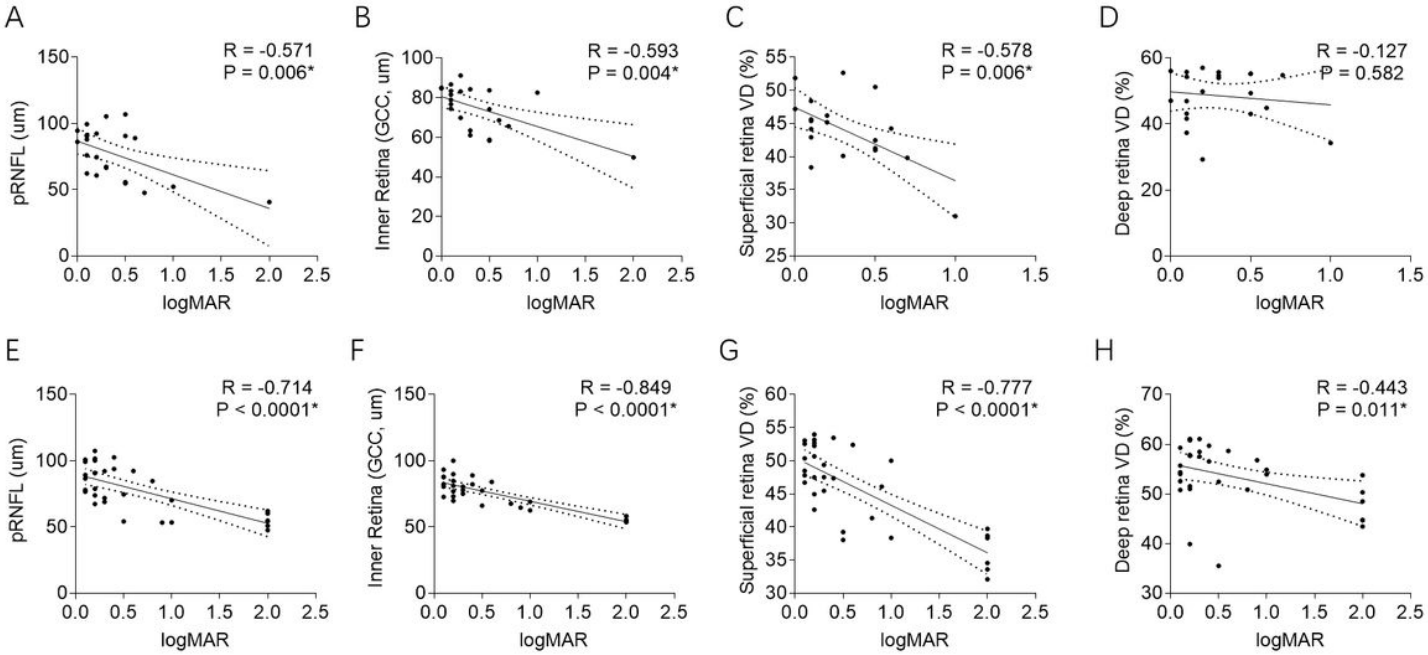

Figure 2

The correlation between retinal structural and microvascular characteristics and visual accuracy. A-D: Scatter plots respectively show the correlation between visual accuracy and pRNFL, inner retina, superficial retinal VD, and deep retinal VD in MOGAD-ON eyes. pRNFL: peri-papillary retinal nerve fiber layer; VD: vessel densities. E-H: Scatter plots respectively show the correlation between visual accuracy and pRNFL, inner retina, superficial retinal VD, and deep retinal VD in AQP4-ON eyes.